Phonons at the surface of the nearly-free-electron metal Al(111): Realization of an ideal surface

A. Lock, J. P. Toennies, and Ch. Wöll
Max-Planck-Institut für Strömungsforschung, Bunsenstrasse 10, D-3400 Göttingen, Federal Republic of Germany

V. Bortolani, A. Franchini, and G. Santoro
Dipartimento di Fisica, Università degli Studi di Modena, via Campi 213/A, I-41000 Modena, Italy
(Received 12 November 1987)

Surface phonons of the nearly-free-electron metal Al(111) have been measured by high-resolution He-atom time-of-flight experiments for four different directions. This is the first surface which shows no evidence for an anomalous resonant mode found on the noble metals and Pt and attributed to a strong ($\approx 50\%$) reduction of surface lateral force constants. By fitting the time-of-flight spectra via a lattice-dynamical simulation the surface interlayer force constant is found to agree to within $\pm 3\%$ with the bulk value and the lateral force constant reduction is less than 20%.

In the last four years it has become possible to measure surface-phonon dispersion curves on metal surfaces using He-atom time-of-flight spectroscopy[1] and electron-energy-loss spectroscopy (EELS).[2] The high resolution of the He-atom scattering has made it possible to observe an unexpected mode in addition to the Rayleigh mode in both the $\bar{\Sigma}\langle 112\rangle$ and $\bar{T}\langle 110\rangle$ directions of the (111) surfaces of Cu,[3] Ag,[1,3] Au,[4] and Pt.[5] This mode has been attributed to an anomalous longitudinal surface resonance resulting from a strong (50–75 %) softening of the lateral force constants[4,6] in the first layer. Although no completely satisfactory theory for this effect has been put forth, the currently favored model attributes the softening to a reduction in the *sp-d* hybridization in the surface layer.[3,6] To test this model and to make data available for a direct comparison with surface-phonon frequencies obtained by *ab initio* pseudopotential calculations, we have carried out the first measurements on a simple nearly-free-electron (NFE) metal surface with an optimalized He time-of-flight spectrometer which allows a precision of 0.1 meV (Ref. 5) in the measurement of dispersion curves. The measurements for Al(111) in the $\bar{\Sigma}$, $\bar{T}$, and—for the first time—two additional directions in between show only the Rayleigh mode. This is the first crystal surface for which there is no evidence for the anomalous longitudinal mode. Because of the increased precision, previously used lattice-dynamical models, which rely on only one or two force constants, are no longer adequate. Thus it has been necessary to use a force field which takes into account very-long-range interactions extending to 10 nearest neighbors to fit both the bulk-phonon dispersion curves and elastic constants. The modification of the radial force constants at the surface is determined from a best fit of the time-of-flight spectra and reveals a negligible change in the vertical interlayer force constant and less than 20% lateral softening, which is consistent with the absence of *sp-d* hybridization in Al. Since *ab initio* pseudopotential calculations of surface-phonon frequencies have already been reported for Al(110),[7] similar calculations for the present system are expected shortly.[8] For comparison with theory, the (111) surface has the advantage that relaxation is small (-0.9%),[9] whereas it is about an order of magnitude larger on Al(110).

The apparatus and measuring procedures are similar to those described previously.[3] The Al crystals were oriented to better than 0.5° and mechanically polished. The final preparation of the surface was done in situ by extensive (>20 h) Ne-ion sputtering and annealing at temperatures up to 800 K. The quality of the surface was first controlled by low-energy electron diffraction (LEED). The Auger spectra measured with a cylindrical-mirror analyzer revealed C and O contaminations of less than 1% of a monolayer. From an analysis of the wide-angle incoherent scattering, the defect density was found to be very low ($<1\%$).[10] Over 500 time-of-flight (TOF) spectra were measured at crystal temperatures of $T=300$ and 150 K.

In Fig. 1 we present a few selected low-temperature TOF spectra for the high-symmetry direction $\bar{T}\langle 110\rangle$. In this direction the highest peaks are associated with a single surface-phonon branch which is attributed to the Rayleigh mode. At $\theta_i=40.91°$ [Fig. 1(c)], the second peak at large energy transfer is split because of two intersections of the kinematic scan curve with the Rayleigh dispersion curve as shown in the inset of Fig. 1. At the next angle the two peaks coalesce, leading to an extraordinary width of the second peak at $\theta_i=40.28°$ and $\hbar\omega=-17.4$ meV [Fig. 1(d)]. This is attributed to the phenomenon of kinematic focusing realized when the kinematic scan curve is tangent to the Rayleigh branch. This phenomenon has been extensively studied in the alkali halides,[11] but has not yet been reported for metals. Its occurrence depends very critically on the scattering angle and, as demonstrated below, provides an especially sensitive test of the phonon dispersion relations.

In general, to determine the surface modification of the force constants by a theoretical fit, we need (1) an accu-

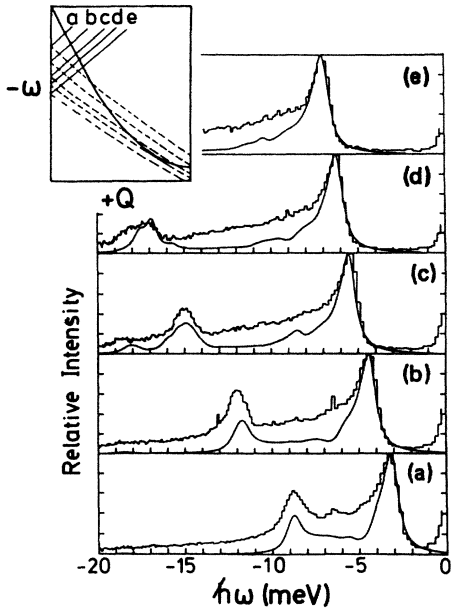

FIG. 1. Comparison of calculated and experimental TOF spectra for Al(111) at $T_{Al}=150$ K, with Q along the $\bar{\Gamma}\langle 110\rangle$ direction, for $E_i=30.4$ meV. The inset presents the Rayleigh dispersion (bold solid line) and the folded kinematic scan curves corresponding to each TOF spectrum. The dashed scan curve is for $-Q$. The smooth curves represent the calculated averaged reflection coefficients, while the histogram represents the experimental data: (a) $\theta_i=42.79°$, (b) $\theta_i=41.83°$, (c) $\theta_i=40.91°$, (d) $\theta_i=40.28°$, and (e) $\theta_i=39.61°$. Note that (d) corresponds to the kinematic focusing condition, where the kinematic scan curve is tangent to the Rayleigh dispersion curve (see inset).

rate parametrization of the force constants of the bulk,[12] (2) a model for the He-atom–surface potential,[13] (3) distorted-wave Born-approximation (DWBA) calculation of the inelastic reflection coefficient,[14,15] and (4) the experimental smearing functions for averaging these reflection coefficients. The available neutron data[16] on Al at 300 K consisting of 100 points and the bulk elastic constants all were fitted using a force-constant parametrization including central interactions up to 10 nearest neighbors (NN's), corresponding to a range of $\sqrt{5}a_0\approx 9.1$ Å, and angular interactions up to four NN's with a precision of better than 1% over the entire Brillouin zone. Note that the analysis of the bulk force constants does indicate the importance of the three-body terms mimicked by the angular force constants δ which give a non-negligible contribution also to the interaction between surface atoms. The large number of nearest neighbors is consistent with previous experience in fitting Al bulk dispersion curves[17,18,19] and is to be compared with the optimal number of nearest neighbors of only four in Ag and Au and six in Ni, Cu, Pd, and Pt.[20,21] The 23 force constants obtained for Al are listed in Table I.

In the slab calculations 90 atomic planes were used to accurately reproduce the density of states and to avoid interference from the two surfaces. A precise fit of the Q dependence of the Rayleigh-mode intensities was achieved with a He-surface repulsive potential, approximated by the Esbjerg-Nørskov procedure.[22] Note that potential parameters affect only the intensities and not the dispersion curves, which are of sole interest here.

On the basis of previous experience the lateral coupling of nearest neighbors in the surface plane and the nearest-neighbor coupling with atoms in the second plane were treated separately and assigned radial force constants $\beta_{\parallel}$ and $\beta_{\perp}$, respectively. A best fit of all the time-of-flight spectra could be achieved for all four directions studied, as shown in Fig. 2 by varying only these two force constants while keeping all the other force constants fixed (Table I). The best-fit force constants of the surface Rayleigh mode are $\beta^s_{\parallel}=\beta^b$ and $\beta^s_{\perp}=1.015\beta^b$. The overall agreement between experiment and theory is very good. The largest disagreement is along the $\langle 112\rangle$ direction between $Q=0.6$ and 0.8 Å^{-1}, while at the zone boundary the agreement is again good. A satisfactory explanation for this deviation is not yet available. Some minor discrepancies between the calculated Rayleigh dispersion curve and the peaks in the He-atom time-of-flight spectra are also present at small Q. An extended theoretical investigation has revealed that at small Q the coupling of He atoms to surface vibrations is dominated by the in-

TABLE I. Bulk force constants obtained from a best fit of the bulk data of Stedman and Nielsen (Ref. 18) measured at 300 K. (α denotes the tangential, β the radial, and δ the angular force constants.) The force constants for the 150-K data differ by less than 1%. The values in parentheses are best-fit force constants if interactions up to two NN's only are included.

n	α_n (ergs/cm^2)	β_n (ergs/cm^2)	$\delta_n/3a_0^2$ (ergs/m^2)
1	1.1727×10^3 (-3.07)	2.6449×10^4 (2.3992×10^4)	-1.1537×10^3 (-7.9966×10^2)
2	1.9564×10^2 ($+3.07$)	2.6924×10^3 (1.4297×10^3)	-5.1585×10^1 (3.6258×10^2)
3	1.1789×10^1	-6.5290×10^2	0
4	-2.0923×10^2	-9.3868×10^1	3.9235×10^2
5	8.2131×10^1	-7.5734	0
6	8.1249×10^1	4.2362×10^2	0
7	7.4504	1.1551×10^2	0
8	-1.0871×10^1	2.0603×10^2	0
9	-7.5627×10^1	1.2813×10^2	0
10	6.4154	3.7503×10^2	0

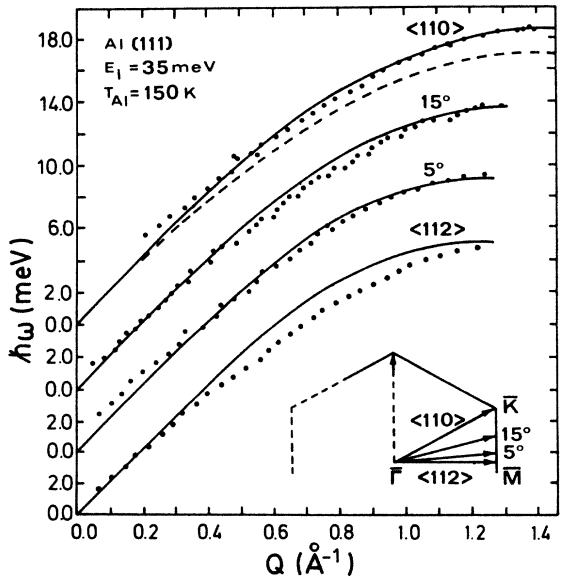

FIG. 2. Comparison of calculated (solid line) and experimental (points) dispersion curves of the Rayleigh mode along the four directions shown in the inset. The solid line is calculated with $\beta_{\parallel}^{s}$ and $\beta_{\perp}^{s}$ adjusted and 10NN interactions, while the dashed line is calculated for a 2NN interaction model (see Table I).

teraction with bulk modes.

A comparison of the best-fit calculations with some of the experimental TOF spectra can be seen in Fig. 1. In the $\bar{T}\langle 110\rangle$ direction the agreement of theory with the experimental locations of the shown two Rayleigh peaks is very good for all scattering angles. Note that at $\theta_i = 40.28°$ the calculated reflection coefficient predicts a single peak at $\hbar\omega = -17.4$ meV with an increased width, in excellent agreement with the experiment. The broadening is related to the behavior of the reflection coefficient, which near kinematic focusing at $E_i = E_i^{\text{foc}}$ behaves as $1/\sqrt{E_i - E_i^{\text{foc}}}$.[23] The inverse square root averaged over all permissible incident energies leads to the widening of the peak. There are still noticeable differences between the theoretical and experimental intensities in the TOF spectra at energy transfers beyond the first peak and especially between the two main peaks, which are not understood. Since the simulation takes full account of the interaction with bulk phonons, these cannot explain the discrepancies, unless possibly the potential used is less successful in describing the coupling to bulk modes at the surface. Multiphonon processes also appear unlikely because their contribution should scale with the ratio of the collision energy to the phonon frequencies, which for Al(111) is smaller when compared to other systems, especially Pt(111),[5] where the multiphonon contribution appears to be small.

To assess the precision of the fit, we evaluate, for the focusing condition of Fig. 1(d), the reflection coefficients by alternately varying either the lateral $\beta_{\parallel}^{s}$ [Fig. 3(a)] or the transverse $\beta_{\perp}^{s}$ [Fig. 3(b)] nearest-neighbor radial force constants with respect to the bulk value β^{b}. From Fig. 3(a) we observe that for $\beta_{\parallel}^{s} = 0.8\beta^{b}$ (dashed curve) the peak related to kinematic focussing disappears entirely. At $\beta_{\parallel}^{s} = 0.5\beta^{b}$ (dotted curve) a slight shoulder corresponding to a longitudinal surface resonance[1,6] becomes visible on the left-hand side of the Rayleigh peak (-10 meV) and is seen more clearly because of kinematic focusing at the $-Q$ intersection (see inset of Fig. 1) at -13 meV. The observed weak dependence on $\beta_{\parallel}^{s}$ of the low-energy Rayleigh peak is explained by its predominant vertical polarization. The change in the frequency of this mode and the appearance of the anomalous longitudinal resonance is observable only for $\beta_{\parallel}^{s} \leq 0.8\beta^{b}$ and thus $\beta_{\parallel}^{s}$ can only be determined to within about 20% with respect to β^{b}.

The high accuracy in measuring the small increase in $\beta_{\perp}^{s}$ compared to the bulk can be explained by the extreme sensitivity provided by the kinematic focusing angles, which in our apparatus can be measured with a digital angle encoder with an absolute precision of $\leq 0.1°$. This is illustrated in Fig. 3(b), where the simulated time-of-flight spectra are shown for different choices of $\beta_{\perp}^{s}$. As one can see, a 5% change of $\beta_{\perp}^{s}$ in both directions away from the best-fit value $\beta_{\perp}^{s} = 1.015\beta^{s}$ produces strong modifications of the kinematical focusing peak. Both an increase and decrease in $\beta_{\perp}^{s}$ lead to significant shifts in peak location to lower energies and reduction in intensities and disappearance of the kinematical focusing peak, and the precision in determining $\beta_{\perp}^{s}$ is estimated to be $\pm 3\%$.

The necessity of using a large number of force constants to fit phonons along all directions in the two-dimensional Brillouin zone is demonstrated by applying the same best-fit scheme reported above to a model, where interactions beyond two NN's are neglected. The dispersion curve obtained with this simplified 2NN model for the $\bar{T}\langle 110\rangle$-symmetry direction is displayed as a dashed line in Fig. 2. It lies considerably below both the experiment and the more extensive calculations. Calculations using a best-fit value for only one single force con-

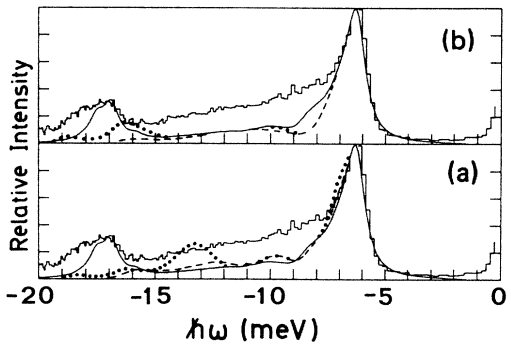

FIG. 3. Comparison of reflection coefficients calculated for different choices of $\beta_{\parallel}^{s}$ and $\beta_{\perp}^{s}$ with the experimental histogram (the same in each panel) of Fig. 1(d). In both panels the solid line is the theoretical calculation with $\beta_{\parallel}^{s} = \beta^{b}$ and $\beta_{\perp}^{s} = 1.015\beta^{b}$. In (a) the effect of modifying $\beta_{\parallel}^{s}$ is shown, where the dashed line is for $\beta_{\parallel}^{s} = 0.8\beta^{b}$ and the dotted line for $\beta_{\parallel}^{s} = 0.5\beta^{b}$. In (b) the dotted line shows the effect of modifying $\beta_{\perp}^{s} = 1.07\beta^{b}$ and the dashed line for $\beta_{\perp}^{s} = 0.97\beta^{b}$.

stant β also lie close to the dashed line. An interpretation based on the results of this oversimplified model, used extensively in the past,[2] would therefore lead to the erroneous conclusion that the surface force constants are strongly modified compared to the bulk.

In summary, we point out that we have been able to fit He-atom TOF spectra without any significant changes in the force constants at the surface by starting from a set of 23 different force constants obtained from a best fit of bulk dispersion curves. From spectra taken near kinematic focusing conditions the nearest-neighbor interlayer force constant $\beta_{\perp}^{s}$ is found to be insignificantly (1.5 ± 3 %) larger than in the bulk, while the nearest-neighbor lateral force constant $\beta_{\parallel}^{s}$ is definitely greater than 80% of the bulk value. In the case of noble and transition metals it was found that a strong weakening of the lateral interaction ranging from $\beta_{\parallel}^{s}\simeq 0.20-0.40\beta^{b}$ for Cu, Au,[4] and Pt to $\beta_{\parallel}^{s}\simeq 0.5\beta^{b}$ for Ag (Ref. 6) was necessary in order to reproduce a strong longitudinal resonance in the continuum of the bulk modes, which was observed as a second anomalous peak in the TOF spectra.

The physical reason for the lack of a lateral softening in aluminum is consistent with our earlier explanation of the lateral softening in the noble and transition metals as being due to *sp-d* hybridization. Obviously, for the NFE metal aluminum, which does not have any *d* shells, *sp-d* hybridization is totally absent. Thus Al(111) is the first surface which does not show a noticeable change in structure and dynamics compared to the bulk.

Recently, *ab initio* calculations were reported for Al(110).[7] Similar calculations are in progress for Al(111),[24] and it will be interesting to compare them with these measurements. Finally these results should also provide a test of a new pseudoparticle model of phonons recently proposed for explaining the surface-phonon anomalies seen in the noble metals.[25]

ACKNOWLEDGMENTS

We want to thank K. P. Bohnen for several discussions. We are grateful to S. Andersson (University of Gothenburg) and K. Christmann (University of Berlin) for the loan of Al crystals, and J. Ernst (Max-Planck-Institut für Strömungsforschung, Göttingen) and J. R. Manson (Clemson University) for a critical reading of the manuscript.

[1]R. B. Doak, U. Harten, and J. P. Toennies, Phys. Rev. Lett. **51**, 578 (1983).

[2]J. M. Szeftel, S. Lehwald, H. Ibach, T. S. Rahman, J. E. Black, and D. L. Mills, Phys. Rev. Lett. **51**, 268 (1983).

[3]U. Harten, J. P. Toennies, and Ch. Wöll, Faraday Discuss. Chem. Soc. **80**, 1 (1985).

[4]V. Bortolani, G. Santoro, U. Harten, and J. P. Toennies, Surf. Sci. **148**, 82 (1984).

[5]U. Harten, J. P. Toennies, Ch. Wöll, and G. Zhang, Phys. Rev. Lett. **55**, 2308 (1985).

[6]V. Bortolani, A. Franchini, F. Nizzoli, and G. Santoro, Phys. Rev. Lett. **52**, 429 (1983).

[7]K. M. Ho and K. P. Bohnen, Phys. Rev. Lett. **56**, 934 (1986).

[8]K. P. Bohnen (private communication).

[9]H. B. Nielsen and D. L. Adams, J. Phys. C **15**, 615 (1984).

[10]A. M. Lahee, J. R. Manson, J. P. Toennies, and Ch. Wöll, Phys. Rev. Lett. **57**, 471 (1986).

[11]G. Brusdeylins, R. B. Doak, and J. P. Toennies, Phys. Rev. B **27**, 3662 (1983).

[12]V. Bortolani, A. Franchini, and G. Santoro, in *Electronic, Dynamics and Quantum Structural Properties of Condensed Matter*, edited by J. T. Devreese and P. van Camp (Plenum, New York, 1985), p. 401.

[13]V. Bortolani, A. Franchini, N. Garcia, F. Nizzoli, and G. Santoro, Phys. Rev. B **28**, 7358 (1983).

[14]V. Bortolani, A. Franchini, F. Nizzoli, G. Santoro, G. Benedek, and V. Celli, Surf. Sci. **128**, 249 (1983).

[15]V. Celli, G. Benedek, U. Harten, J. P. Toennies, R. B. Doak, and V. Bortolani, Surf. Sci. **143**, L376 (1984).

[16]R. Stedman and G. Nilsson, Phys. Rev. **145**, 492 (1966).

[17]G. L. Squires, *Inelastic Scattering of Neutrons in Solids and Liquids* (IAEA, Vienna, 1962), Vol. II, p. 55.

[18]S. H. Vosko, R. Taylor, and G. H. Keech, Can. J. Phys. **43**, 1187 (1965).

[19]G. Gilat and R. M. Nicklow, Phys. Rev. **143**, 487 (1966).

[20]A. Franchini, Ph.D. dissertation, University of Modena, 1985/86 (unpublished).

[21]The explanation for the large number of nearest neighbors in Al may be related to the especially high density of electrons, which leads to a particular strong electron-ion interaction.

[22]N. Esbjerg and J. K. Nørskov, Phys. Rev. Lett. **45**, 807 (1980).

[23]S. W. Lovesey, *Theory of Scattering from Condensed Matter* (Clarendon, Oxford, 1984), Vol. I, p. 114.

[24]A. G. Eguiluz, Phys. Rev. B **35**, 5473 (1987).

[25]C. S. Jayanthi, H. Bilz, W. Kress, and G. Benedek, Phys. Rev. Lett. **59**, 795 (1987).